

Article

Snakeskin-Inspired 3D Printable Soft Robot Composed of Multi-Modular Vacuum-Powered Actuators

Seonghyeon Lee ^{1,†}, Insun Her ^{2,†}, Woojun Jung ¹ and Yongha Hwang ^{1,*} ¹ Department of Control and Instrumentation Engineering, Korea University, Sejong 30019, Republic of Korea² Department of Electro-Mechanical Systems Engineering, Korea University, Sejong 30019, Republic of Korea

* Correspondence: hwangyongha@korea.ac.kr

† These authors contributed equally to this work.

Abstract: A modular soft actuator with snakeskin-inspired scales that generates an anisotropic friction force is designed and evaluated in this study. The actuator makes it possible to fabricate soft robots that can move on various surfaces in the natural environment. For existing modulus soft robots, additional connectors and several independent pneumatic pumps are required. However, we designed precise connection and snake-scale structures integrated with a single pneumatic modular actuator unit. The precise structure was printed using a DLP 3D printer. The movement characteristics of the soft robot changed according to the angle of the scale structure, and the movement distance increased as the number of modular soft actuator units increased. Soft robots that can move in operating environments such as flat land, tubes, inclined paths, and water have been realized. Furthermore, soft robots with modularization strategies can easily add modular units. We demonstrate the ability to deliver objects 2.5 times heavier than the full weight of the soft robot by adding tong-like structure to the soft robot. The development of a soft robot inspired by snakeskin suggests an easy approach to soft robots that enables various tasks even in environments where existing robots have limited activity.

Keywords: modular soft robot; snakeskin inspiration; keeled scales; anisotropic friction force; vacuum-powered actuators; DLP 3D printing



Citation: Lee, S.; Her, I.; Jung, W.; Hwang, Y. Snakeskin-Inspired 3D Printable Soft Robot Composed of Multi-Modular Vacuum-Powered Actuators. *Actuators* **2023**, *12*, 62. <https://doi.org/10.3390/act12020062>

Academic Editor: Hamed Rahimi Nohooji

Received: 9 January 2023

Revised: 27 January 2023

Accepted: 29 January 2023

Published: 31 January 2023



Copyright: © 2023 by the authors. Licensee MDPI, Basel, Switzerland. This article is an open access article distributed under the terms and conditions of the Creative Commons Attribution (CC BY) license (<https://creativecommons.org/licenses/by/4.0/>).

1. Introduction

Biological inspiration designs that mimic biological structures enable efficient movement in cluttered or unstructured environments such as medical care, search and rescue, and disaster response, as well as efficiency in tasks that require being in close contact with people [1,2]. Recently, soft robots have been constructed to mimic the structures of various mollusks [3]. In particular, a driving mechanism simulating the movement of snakes or caterpillars has shown effective movement in environments that impose motion constraints on wheeled or legged robots [4,5]. The caterpillar moves in one way using a controllable proleg and thoracic leg [6,7]. Snakes, despite having no limbs, can move by pulling forward scales of tile-like shapes that generate anisotropic friction and constrict the flexible body [8,9].

Various manufacturing methods, such as the reproduction molding process [10], rotary casting [11], screen printing [12], and 3D printing [13], have been proposed for manufacturing soft robots inspired by the living body [14,15]. In particular, owing to the development of 3D printing technology, the production of complex 3D structures by printing various polymer materials with high resolution has become possible [16]. Fused deposition modeling (FDM) technology, one of the most typical 3D printing methods, allows for the manufacture of a pneumatic actuator at a relatively low price using a thermoplastic elastomer (TPE) and thermoplastic polyurethane (TPU) material with a shore hardness of 70–80 A, which is more flexible than ordinary hard lactic acid (PLA) and acrylonitrile butadiene styrene (ABS) materials [17,18]. However, FDM 3D printers

have limited resolution depending on the nozzle diameter (minimum: 0.1 mm); therefore, the thickness of the thin film constituting the actuator must be at least three times the size of the nozzle [19]. Direct ink writing (DIW) technology has been used to manufacture pneumatic actuators by extruding polymer materials such as silicone elastomers rather than filament-type materials [20,21]. However, similar to the FDM, the resolution is limited depending on the nozzle diameter and is inversely proportional to the build speed [19]. Polyjet technology is a technique for selectively spraying and depositing droplets of raw material onto the surface and has been used in the development of soft actuators using multi-material 3D printers that can print mixtures of rubber-like, hard, and soft materials [22,23]. However, as commercially manufactured inkjet materials are still limited, and designing chemicals capable of droplet formation and deposition and replacing printer heads is expensive, polyjet technology has drawbacks [19]. Stereolithography apparatus (SLA) technology selectively photopolymerizes and stacks liquid resins using a laser and can be used to develop micro-actuators because it can quickly and easily print high-resolution materials [24,25]. However, to date, multiple materials cannot be printed in a single printing sequence [26]. In addition, microsized soft actuators and fluid devices have been manufactured using casting polymer materials and chemically removing molds by printing molds with a 3D wax printer with a microsized resolution, rather than direct printing of polymer materials. However, mold removal technology using a 3D wax printer requires a relatively longer process time than a 3D printing method that directly prints polymer materials owing to the additional manufacturing process required to remove supporter materials and cure thermosetting polymers [27,28].

Soft pneumatic actuators can be divided into positive- and negative-pressure actuators. Positive-pressure soft actuators are inflated by injecting air-like fluid during operation, while negative-pressure soft actuators vacuum the interior and contract the volume of the actuator. Such negative-pressure actuators are preferred over positive-pressure actuators when performance limitations are required in terms of output force and deformation [29]. Compared to expanding positive-pressure actuators, negative-pressure actuators are reduced in volume during operation, making them unsuitable for use in narrow spaces and safe for use in vulnerable places such as the interior of people [30]. In addition, it is safer and less likely to fail than a positive-pressure soft actuator that expands during activation and is prone to breakage at high pressures [31].

The convenience of 3D structure manufacturing through 3D printing makes it easy to implement a modular strategy that disassembles one product into units that can be configured, decomposed, replaced, and managed easily [32]. This makes it easy to rebuild various forms to satisfy the requirements of a given environment and task. An assembly module system was used to implement soft robots such as gripping robot arms [33] and biomimicry moving robots [34] whose implementation is difficult with a single actuator. The reconfigurable module system can quickly replace units of various functions compared with single functions, enabling the implementation of a general-purpose soft robot. Using a reconfigurable module system, Zhang developed a soft robot capable of configuring worm-type, cross-legged quadrupedal walks, and hexapods [35]. Jiao developed robots with various functions such as gripping, bottle opening, crawling, and pipe climbing [36]. These modular soft robots adopt a method of applying pneumatic pressure to each of the connected modular actuator units, thus requiring several pneumatic pumps that are independently activated to perform the task [37,38]. On the other hand, Tawk developed a single pneumatic modular soft actuator to demonstrate the implementation of soft robots capable of the movement and rapid replacement of units with various functions. However, because parts made of other materials such as small rare-earth rings, rod magnets, and small plastic tubes are required to connect modular actuators, the fabrication process is complicated and limited to scale-down owing to manual assembly [39].

We have herein demonstrated a micro soft mobile robot that is as easy, simple, and free from breakage as possible. The soft robot is printed to a flexible resin using a high-resolution 3D printer using the digital light processing (DLP) method, which is a commercially avail-

able SLA method and is then completed after a typical postprocessing process. For simple fabrication, the robot was designed to have a shape that does not have a supporting structure, which is required for the implementation of complex structures in 3D printing technology. Through such 3D printing technology, precise connection structure can be produced, and a modularization strategy was applied to the robot. By repeatedly connecting basic modularized units of the same shape to form one robot that moves forward, composing the body of commercially available flexible resins is easy and simple. This is because even if a part of the body is defective during production, recreating the entire body is not necessary, and only one modular unit needs to be produced. In addition, a modular soft-moving robot capable of multiple connections can vary its length and mobility of the soft robot depending on the number of units connected by the user due to its modular structure. In particular, the modular soft actuator operates using a single pump connected to a single tube. As negative pressure is used, the actuator is free from the risk of bursting or leaking pressure compared with the method of operating by expansion due to positive pressure. To this end, it is designed to move only with linear contraction and restoration using a snakeskin structure application that generates an anisotropic friction force on the soft robot. The moving characteristics of a modularized snakeskin soft robot (MSSR) using a single pneumatic method have been experimentally confirmed according to design parameters, and its operation in practical operating environments, such as bent tubes and inclined paths, has been proven.

2. Concept and Design

2.1. Bioinspiration from the Snakeskin

The shape and size of scales on the skin of snakes vary depending on their type, habitat, and ecology. We designed MSSR scales inspired by the distinct keeled scales of *Atheris hispida*, also known as the Bush viper, which lives in rainforests, as shown in Figure 1a. Bush vipers, which can move in various environments (including trees, plant leaves, rocks, and soil) with anisotropic friction on surfaces of various roughness, have evolved efficiently; as a result, they have a distinct keeled appearance compared to other snake scales [40,41]. To realize such keeled scales, the 3D design of each scale was designed to ensure that the front surface in the moving direction would be slippery and the back surface in the opposite direction would be fixed. To make each of the designed scales converge at the center point of one of the pentagonal corners and form an anchor structure in the opposite direction of movement, we trimmed the back face into a triangular column. In such a design, a slippery smooth surface is formed on the front surface, a fixed anchor surface is formed on the rear surface, and the shape is similar to that of a snake scale, generating an anisotropic friction force on the floor.

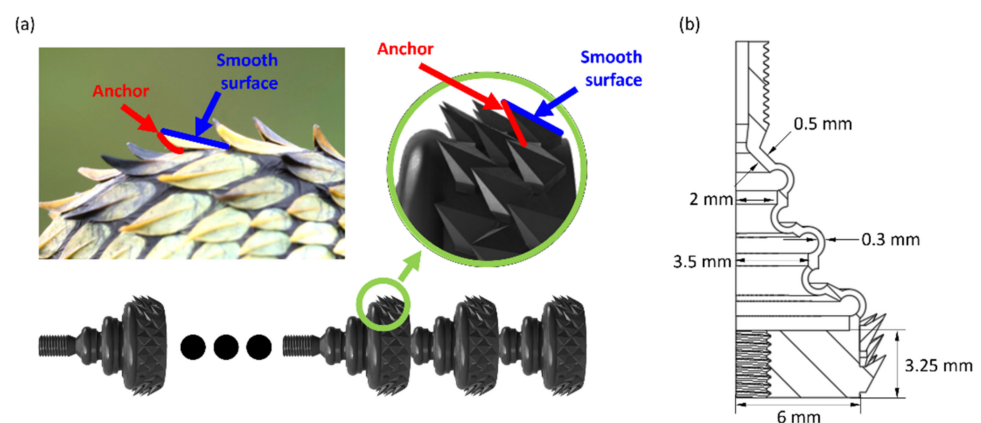


Figure 1. Schematic of MSSR. (a) MSSR's structure inspired by Bush viper's distinct keeled scales. (Photo courtesy of Mark Kostich, Adobe Stock images). (b) Cross-section (axial symmetry) and parameter values of soft actuator design for DLP 3D printing without supporting structures.

2.2. Structure Design and Fabrication of the MSSR

A flexible resin (F80, Dongguan Godsaid Technology, Dongguan, Guangdong Province, China) was used to print the pneumatic soft actuator using a 3D printing method. The flexible resin has a shore hardness range of 50–60 A; thus, it exhibits high flexibility and resilience, and is suitable for making soft actuators. We empirically verified the printing performance of a recently commercialized DLP 3D printer (Sonic Mini 8 K, Phrozen Technology, Hsinchu City, Taiwan) with a 22- μm resolution and the properties of the tearable resin by creating a modular unit with as thin a wall as possible using 3D CAD (Fusion 360, Autodesk, Mill Valley, CA, USA). The thickness and dimensions of the unit are shown in Figure 1b. As support material different from the structural material cannot be used in a DLP printer for printing only a single material, a modular soft actuator unit was designed in a shape where the volume gradually decreased as the modular soft actuator unit goes upward and thus requires no internal supporting structure. A male connector and a female connector for assembling units were arranged on the top and bottom surfaces of the basic units so that multiple units can be easily connected. When we designed the connectors of the two parts, we empirically checked the diameters that can be connected without air leaking. Values of 0.125 inches for the male and 0.1325 inches for the female screw diameter were selected, and vacuum pressure was applied up to 15 kPa after sealing, but no problem was observed. An empty channel existed at the center of the male connector to apply air pressure to the actuator. Considering such conditions, we set the resin printing parameters: layer height (50 μm), exposure time (3 s), and rest time after retraction (4 s). After the completion of printing of each unit, each unit was removed from the platform of the 3D printer, and the stuck resin that was not hardened was removed by placing it in ethanol and stirring for 20 min. The unit was then placed in a UV curing device under a vacuum for 300 s for final curing. By connecting the circular symmetric modular actuator unit manufactured by 3D printing, the two design connectors of the integrated body engage through the thread so that air does not leak from the connection when air pressure is applied. Only the actuator unit placed at the front of the moving direction was designed without a female connector; thus, the free space of the MSSR was sealed. The back surface of the unit, arranged at the rear of the moving direction, was connected to a pressure pump to drive through a silicone tube.

2.3. Mechanism for Operation

The MSSR has a collapsible funnel design that folds vertically in the direction of travel, as shown in Figure 2a, to employ the negative-pressure system. A pneumatic soft actuator of the positive pressure type may be damaged by excessive expansion and may also damage the surrounding environment. To prevent such problems, a negative-pressure system that does not excessively expand was selected. The folding funnel structure used in the MSSR was designed to fold the wall without expanding or contracting; it was composed of flexible resin, so it could expand and contract in when operated under positive pressure. However, owing to the thin wall, the wall of MSSR may be torn or damaged if it expands under excessive pressure.

To effectively contract the actuator by folding the wall with vacuum pressure, a structure with an arc-shaped cross-section for each part where the wall surface was folded, as shown in Figure 2b, was added to the folding funnel structure. We compared the structure of the actuator with and without an arc joint through a finite element analysis using the solid mechanics modules of the multiphysics analysis program (COMSOL/Multiphysics, COMSOL, Burlington, MA, USA). First, a 3D actuator with a structure similar to that of an existing folding funnel was designed, and a structure containing an arc joint was added. The material properties were set at Young's Modulus 2.159 MPa in consideration of Shore-A hardness of F80 resin [42]. In addition, tensile strength (3.5 MPa), tear strength (9.7 kN/m), elongation at break (159%), and viscosity (2300 mPa·s) were used from the datasheet of F80. A Poisson ratio of material was set by referring to a general flexible resin physical property of 0.49 [43]. The density was measured from the volume and mass of the printed

resin structure. By applying the same negative pressure inside each actuator, the changes in the two 3D structures and the displacement of one point on the top surface were analyzed; subsequently, the 3D printed actuator was air pressure tested and measured. By comparing the results of the pneumatic test of actuators manufactured in the two designs in Figure 2c with pressure-induced displacement change, we observed that actuators with arc joints showed 1041.6% higher displacement than actuators without arc joints and had a 9.3% fine error with simulation analysis. This is because the arc joints facilitate the folding of the actuator wall and reduce the elastic force generated by the folding.

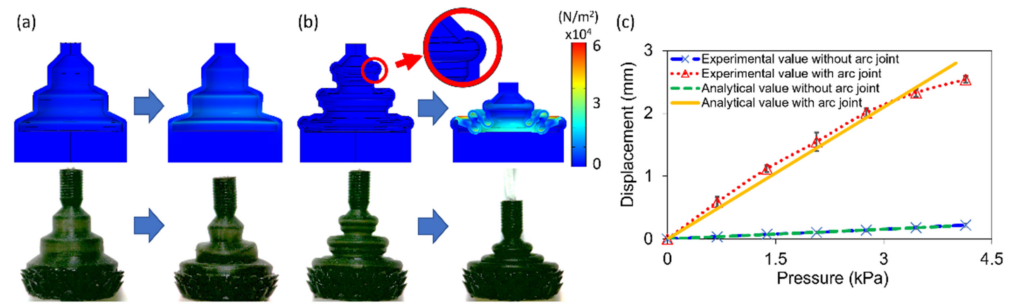


Figure 2. FEM analysis results and the actuator with vacuum applied for characterization of the soft actuator: (a) Collapsible funnel-shaped design. (b) Arc joint design. (c) Displacement of actuators depending on applied pressure.

Figure 3a illustrates the progression mechanism of MSSR. In the process of contracting or returning to the initial state, when five soft actuator units were connected, the snake scales of each unit generated different frictional forces from the floor. When contracting initially, negative pressure was applied to the MSSR, and the scales of the rear unit of the moving direction based on the center of gravity demonstrated a phenomenon wherein a smooth surface with low friction force brushed the floor and slipped. In the front unit, on the contrary, the anchor part of the scales was fixed by generating high friction force with the floor. Accordingly, the front unit showed fixed or low movement, and the rear unit slid and exhibited high mobility. If the contracted amount of air was placed inside again, it returned to its original state; however, in contrast to the contraction, the rear unit was fixed, and the front unit slid, indicating a phenomenon wherein the whole body moved forward. By repeating one series of cycles, the MSSR to which multiple units were connected could proceed as intended. After connecting a micro silicone hose (inside diameter: 0.4 mm; outside diameter: 1.2 mm) to the manufactured unit, such as Figure 3b, an air pressure test with a syringe confirmed that it moved in the same manner (Video S1).

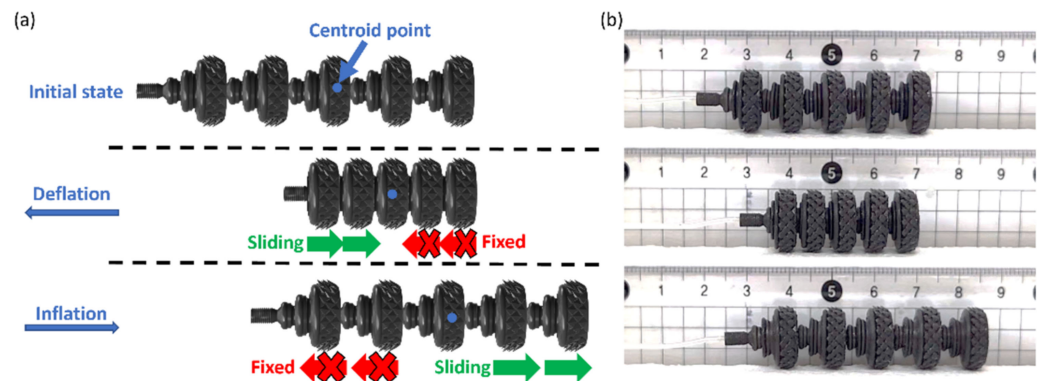


Figure 3. Locomotion model of MSSR. (a) Movement mechanism of MSSR with five modular soft actuator units connected. (b) Images of the moving MSSR during one cycle.

3. Discussion

We considered the effect of the angle formed between the rear anchor part of the snake scales and horizontal axis, as shown in Figure 4. As shown in Figure 4a, actuator units with scales between the horizontal axes and anchor parts ranging from 30° to 60° were manufactured, and their moving capabilities on wood and paper substrates were compared with MSSRs with five connected units. The term “iteration” denotes the number of cycles that completely contract and return to the original state. As seen in Figure 4b, the MSSR on the paper substrate MSSRs with 30° scales demonstrated the highest displacement of the four designs. On the wood substrate, the MSSR at the 50° scale demonstrated the highest displacement, as shown in Figure 4c. Paper substrates with lower roughness than wooden plates enabled us to confirm the characteristics of the MSSR movement on a smooth surface. The changes in movement characteristics of MSSR on 400 grit and 100 grit sandpaper with $13.21\ \mu\text{m}$ and $24.93\ \mu\text{m}$ roughness are shown in Figure 4d,e, respectively. In addition, to confirm the anisotropic friction force of each scale generated on the surface of the paper, wooden, and sandpaper boards, the static friction coefficient was determined, as shown in Table 1. It shows the difference between the forward friction coefficient ($\mu_{S,\text{forward}}$) and the backward friction coefficient ($\mu_{S,\text{backward}}$) according to the scale angle and the substrate material. The differences in the friction coefficient and displacement of the MSSR for each substrate showed the same tendency. Therefore, the characteristics of the displacement varied depending on the roughness of the floor surface when the MSSR moved. As the anchor surface is hardly fixed on the smooth surface, the unit needs to have fixed slips. Owing to these characteristics, replacing actuator units with appropriate snake-scale angles considering the roughness of the environment in which the MSSR operates is appropriate. Module replacement depending on the situation is simple and easy owing to the module strategy.

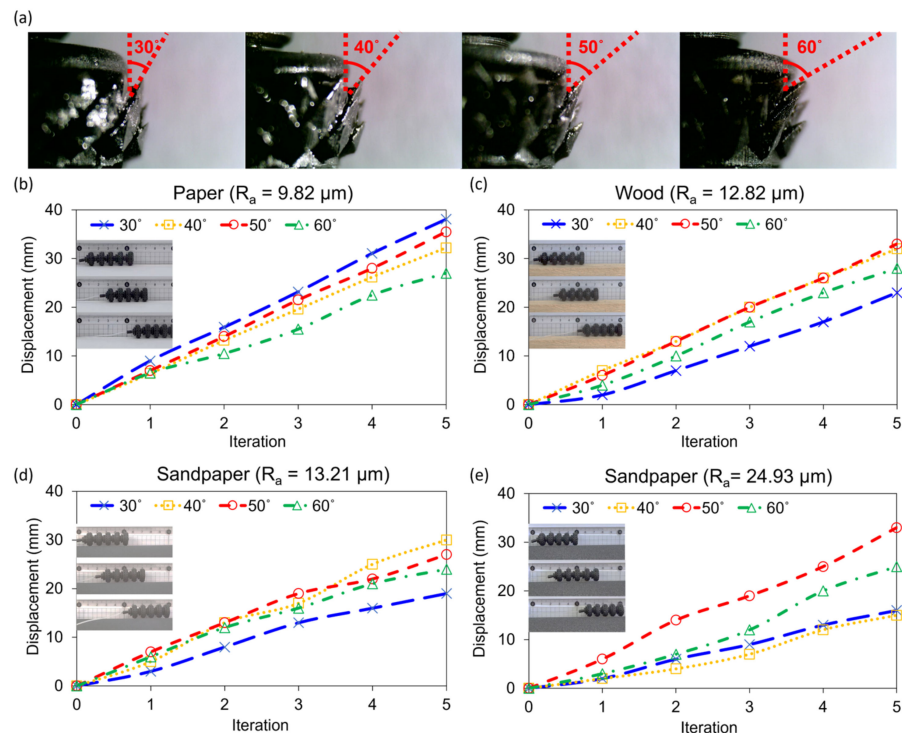


Figure 4. Characteristics depending on the angle between the horizontal axis and the anchor plane of the snake scale structure. (a) Close-up image of snake scale structure designed from 30° to 60° (red dotted line representing the angle of the anchor face of the calculated 3D design). Displacement according to the operating cycle of MSSR, which is made of five modular soft actuator units, on (b) paper, (c) wood surfaces and sandpapers with two different surface roughness ((d) $13.21\ \mu\text{m}$, (e) $24.93\ \mu\text{m}$).

Table 1. Differences between backward and forward friction coefficients ($\mu_{S,forward} - \mu_{S,backward}$) according to snake scale structure angle.

Angle	30°	40°	50°	60°
Wood ($R_a = 12.82$)	0.14	0.28	0.30	0.20
Paper ($R_a = 9.82$)	0.23	0.06	0.17	0.03
Sandpaper ($R_a = 13.21$)	0.25	0.59	0.48	0.38
Sandpaper ($R_a = 24.93$)	0.18	0.15	1.02	0.67

As the number of modular actuator units increased, the displacement per iteration generated in the process of contraction or returning to the initial state increased, as shown in Figure 5. This is because the total displacement increases in proportion to the number of units that are resistant when pushed backward but easily slip forward. However, in a slippery material such as glass, where an anisotropic frictional force due to the scale structure is not generated, the change in displacement does not increase, even when the number of units increases. The experiment was conducted on a paper towel with a rough surface prone to anisotropic frictional forces.

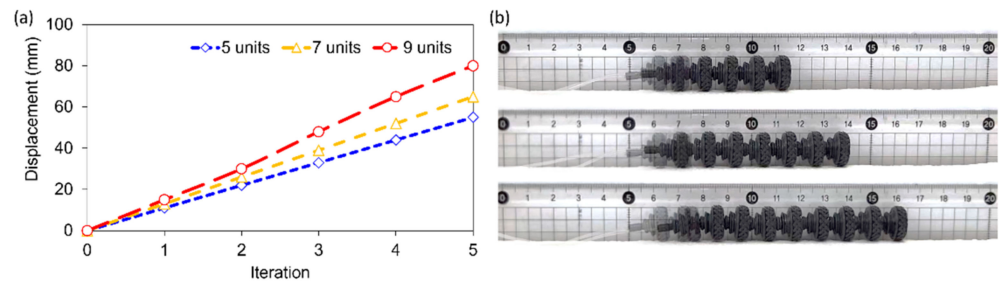


Figure 5. Characteristics according to the number of modular soft actuator units. (a) Displacement changes according to the operation cycle of MSSR with different number of units on the rough surface paper towel that easily has anisotropic frictional force. (b) Initial and final positions of the captured MSSR after one cycle.

The advantage of modular robots is that they can replace units with various functions. In particular, to put mobile soft robots into practical use, heavy parts and cargo can be transported compared with the main body. Therefore, we added units in the shape of tongs at the front of the MSSR that are designed to fix a payload that moves with the unit, as shown in Figure 6 and Video S2. As the number of connected units increased, the weight of the payload that could be moved without MSSR bending also increased. We demonstrated that if there are 11 units, up to 2.5 times the weight of the MSSR can be moved as a payload. This is because as each unit increases, the total friction force generated between the anchor surface of the scale and the bottom increases compared with the gravity caused by the weight and the actuator itself. If the MSSR exceeds the weight of the payload it can push, it will not move forward as it will bend its entire body, or all units will slip.

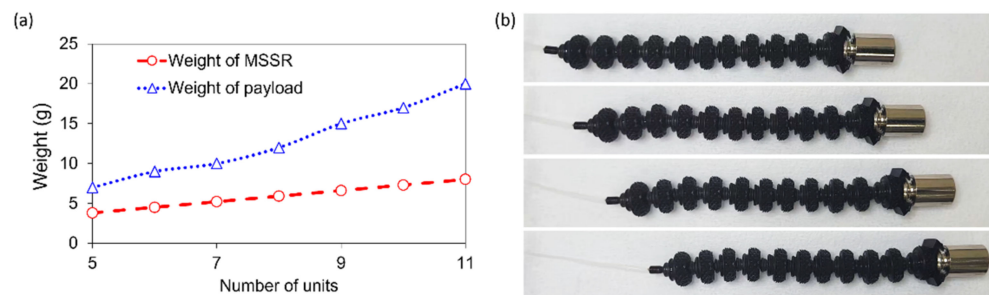


Figure 6. MSSR capable of delivering payload. (a) Change in payload weight that can be moved according to the number of units by adding a tong-type unit. (b) Images captured according to the cycle of delivering a weight 2.5 times the weight of the entire MSSR.

Soft robots that can move without arms and legs are suitable for operation in narrow environments such as pipelines. Therefore, the MSSR has a cylindrical design that can be moved even in a tubular space. We demonstrated MSSR movement with soft transparent PVC tubes, as shown in Figure 7 and Video S3. In addition, Figure 7a shows that it could successfully pass through a bent tube. This demonstrates the strength of the soft actuator, allowing the MSSR unit to operate in a bent state by being made of flexible resin. Figure 7b shows that the MSSR can not only move smoothly in curved tubes but also in S-shaped tubes. The technology of soft robots in structures inspired by snake skins shows the practicality of advanced-level operations in living bodies through 3D printer technology, and supports high-resolution biocompatible material printing in the future.

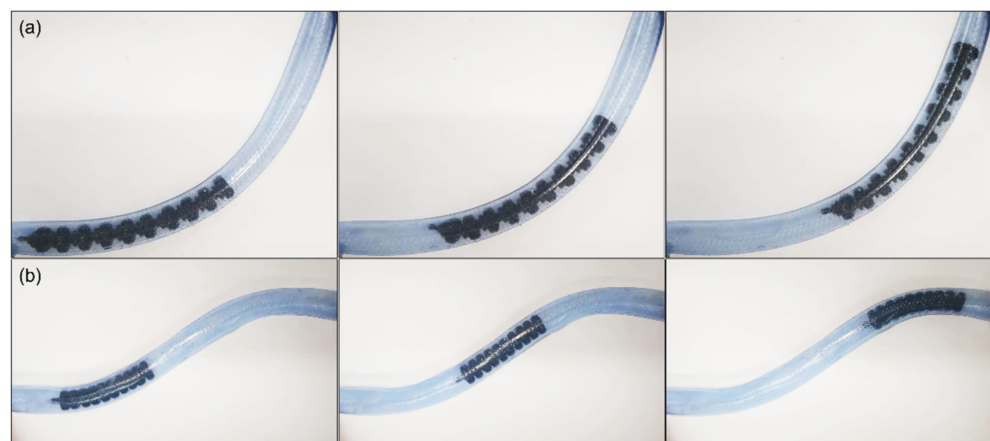


Figure 7. Demonstration of MSSR in a transparent PVC tube. Images captured according to the period of images captured in the (a) bent tube and (b) S-curved tube.

Soft robots should not only be able to operate in planes or tubes but also in a variety of environments. In particular, the natural environment has hill-like terrain with slopes, which can limit movement. Accordingly, the movement of the soft robot on a substrate with different slopes, as shown in Figure 8a, was demonstrated. However, on a substrate where sufficient friction force is not generated, the entire soft robot slips according to the inclination, and the soft robot cannot move forward. In the slope of the paper towel surface, MSSR showed a maximum angle of 30° . At the slope angle of 30° , the moving distance of one cycle of the MSSR was reduced by 33.33% compared to the untilted plane because sliding due to gravity in the slope tends to reduce the moving distance. In addition, in the natural environment, pools of water may occur on flatlands depending on weather or ecology. Such humid environments can cause fatal failures in electrically operated robots. The MSSR is suitable for underwater operation because leakage of internal and external fluid does not occur through the engagement of the thread of the 3D printed connection. Figure 8b demonstrate the mobility of the MSSR underwater. An MSSR, whose interior is filled with air, floats on the surface by buoyancy, but by pressing water pressure with a syringe when the interior is filled with water, anisotropic movement is shown in the same manner as in a flat surface. The speed of movement in the water decreased by 55.88% compared to that of paper towels because there is a drag force of water. Mobility in such environments widens the scope of the environment in which modular units with various functions can perform tasks.

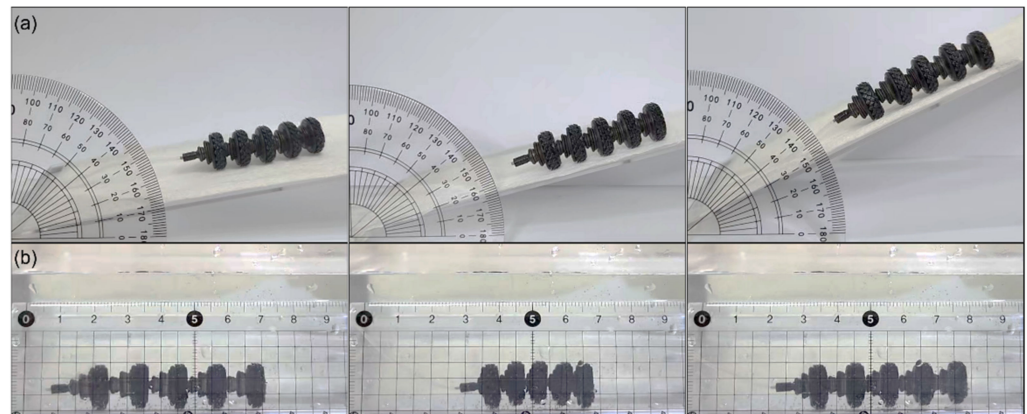


Figure 8. Locomotion of MSSR under different conditions. (a) Demonstration of movement along the slope of the paper tower surface. (b) Captured pictures according to the operating cycle of the MSSR under water.

4. Conclusions

In this study, a modular soft robot was designed and manufactured based on snake scales to enable movement using a single pneumatic actuator. The transfer characteristics of the MSSR by the structure imitating the keeled scales that generate anisotropic friction in various environments were confirmed through changes in the angle with horizontal lines and the number of units of scales. In addition, a tong-type unit was added to confirm the advantage of the modular robot operating by adding modular units with various functions. In the case of adding the tong structure, when the number of units is 11, it can deliver more than 2.5 times the weight of the main body of the MSSR. The MSSR, which is made of flexible resin, demonstrated the advantages of flexible robots by demonstrating bending and moving in cylindrical, curved, and S-shaped tubes. In addition, demonstrating the movement of the robot on slopes and in water showed the possibility of mobility in various environments. In future research, pneumatic actuators will be added to both sides of the module in the head of the robot to allow a smooth change of direction of the MSSR. This diversity of operating environments demonstrates the possibility of developing a soft robot that not only allows robots to move in difficult environments where robots with arms and legs are restricted but also allows for search, rescue, exploration, and inspection work through simple unit replacement. The module was repeatedly tested 10,000 times at constant pressure to confirm that there was no reliability issue. In addition, it was confirmed that the displacement decreased by 3.34% on average at the same pressure using MSSR samples that were left at room temperature for 7 days and 80 days, respectively. This shows that there is no drawback due to material properties. Subsequently, with the development of 3D printing, we believe that microsize implementation and chemically and biologically stable materials can be utilized within the scope of medical and biological fields.

Supplementary Materials: The following supporting information can be downloaded at: <https://www.mdpi.com/article/10.3390/act12020062/s1>; Video S1: Operation of the MSSR with five modular soft actuator units connected; Video S2: Demonstrated delivery of a payload 2.5 times heavier than the full MSSR weight; Video S3: Repeated operation of MSSR in the curved tube and S-curved tube.

Author Contributions: Conceptualization, S.L., I.H., W.J. and Y.H.; methodology, S.L., W.J. and Y.H.; validation, S.L., I.H. and Y.H.; writing—original draft preparation, S.L. and I.H.; writing—review and editing, Y.H.; visualization, I.H. and W.J.; supervision, Y.H.; project administration, Y.H. All authors have read and agreed to the published version of the manuscript.

Funding: This research was supported by the National Research Foundation of Korea (NRF), funded by the Korean Government (MIST) under Grant NRF-2022R1F1A1074083, and the “Regional Innovation Strategy (RIS)” through the NRF, funded by the Ministry of Education under Grant 2021RIS-004.

Institutional Review Board Statement: Not applicable.

Informed Consent Statement: Not applicable.

Data Availability Statement: The data presented in this study are available on request from the corresponding author.

Conflicts of Interest: The authors declare no conflict of interest.

References

1. Trivedi, D.; Rahn, C.D.; Kier, W.M.; Walker, I.D. Soft robotics: Biological inspiration, state of the art, and future research. *Appl. Bion. Biomech.* **2008**, *5*, 99–117. [\[CrossRef\]](#)
2. Kim, S.; Laschi, C.; Trimmer, B. Soft robotics: A bioinspired evolution in robotics. *Trends Biotechnol.* **2013**, *31*, 287–294. [\[CrossRef\]](#) [\[PubMed\]](#)
3. Nurzaman, S.G.; Iida, F.; Margheri, L.; Laschi, C. Soft robotics on the move: Scientific networks, activities, and future challenges. *Soft Robot.* **2014**, *1*, 154–158. [\[CrossRef\]](#)
4. Wang, C.; Puranam, V.R.; Misra, S.; Venkiteswaran, V.K. A Snake-Inspired Multi-Segmented Magnetic Soft Robot Towards Medical Applications. *IEEE Robot. Autom. Lett.* **2022**, *7*, 5795–5802. [\[CrossRef\]](#)
5. Zhang, B.; Fan, Y.; Yang, P.; Cao, T.; Liao, H. Worm-Like Soft Robot for Complicated Tubular Environments. *Soft Robot.* **2019**, *6*, 399–413. [\[CrossRef\]](#)
6. Trimmer, B.; Issberner, J. Kinematics of soft-bodied, legged locomotion in *Manduca sexta* larvae. *Biol. Bull.* **2007**, *212*, 130–142. [\[CrossRef\]](#)
7. Niu, H.; Feng, R.; Xie, Y.; Jiang, B.; Sheng, Y.; Yu, Y.; Baoyin, H.; Zeng, X. MagWorm: A Biomimetic Magnet Embedded Worm-Like Soft Robot. *Soft Robot.* **2021**, *8*, 507–518. [\[CrossRef\]](#)
8. Hu, D.L.; Nirody, J.; Scott, T.; Shelley, M.J. The mechanics of slithering locomotion. *Proc. Natl. Acad. Sci. USA* **2009**, *106*, 10081–10085. [\[CrossRef\]](#)
9. Marvi, H.; Cook, J.P.; Streator, J.L.; Hu, D.L. Snakes move their scales to increase friction. *Biotribology* **2016**, *5*, 52–60. [\[CrossRef\]](#)
10. Shepherd, R.F.; Ilievski, F.; Choi, W.; Morin, S.A.; Stokes, A.A.; Mazzeo, A.D.; Chen, X.; Wang, M.; Whitesides, G.M. Multigait soft robot. *Proc. Natl. Acad. Sci. USA* **2011**, *108*, 20400–20403. [\[CrossRef\]](#)
11. Polygerinos, P.; Lyne, S.; Wang, Z.; Nicolini, L.F.; Mosadegh, B.; Whitesides, G.M.; Walsh, C.J. Towards a soft pneumatic glove for hand rehabilitation. In Proceedings of the 2013 IEEE/RSJ International Conference on Intelligent Robots and Systems, Tokyo, Japan, 3–7 November 2013; pp. 1512–1517.
12. Yeo, J.C.; Yap, H.K.; Xi, W.; Wang, Z.; Yeow, C.-H.; Lim, C.T. Flexible and Stretchable Strain Sensing Actuator for Wearable Soft Robotic Applications. *Adv. Mater. Technol.* **2016**, *1*, 1600018. [\[CrossRef\]](#)
13. Gul, J.Z.; Sajid, M.; Rehman, M.M.; Siddiqui, G.U.; Shah, I.; Kim, K.-H.; Lee, J.-W.; Choi, K.H. 3D printing for soft robotics—A review. *Sci. Technol. Adv. Mater.* **2018**, *19*, 243–262. [\[CrossRef\]](#)
14. Schmitt, F.; Piccin, O.; Barbé, L.; Bayle, B. Soft Robots Manufacturing: A Review. *Front. Robot. AI* **2018**, *5*, 84. [\[CrossRef\]](#)
15. Dong, X.; Luo, X.; Zhao, H.; Qiao, C.; Li, J.; Yi, J.; Yang, L.; Oropeza, F.J.; Hu, T.S.; Xu, Q.; et al. Recent advances in biomimetic soft robotics: Fabrication approaches, driven strategies and applications. *Soft Matter* **2022**, *18*, 7699–7734. [\[CrossRef\]](#)
16. Miller, J.S.; Stevens, K.R.; Yang, M.T.; Baker, B.M.; Nguyen, D.-H.T.; Cohen, D.M.; Toro, E.; Chen, A.A.; Galie, P.A.; Yu, X.; et al. Rapid casting of patterned vascular networks for perfusable engineered three-dimensional tissues. *Nat. Mater.* **2012**, *11*, 768–774. [\[CrossRef\]](#)
17. Yap, H.K.; Ng, H.Y.; Yeow, R.C.-H. High-Force Soft Printable Pneumatics for Soft Robotic Applications. *Soft Robot.* **2016**, *3*, 144–158. [\[CrossRef\]](#)
18. Hu, W.; Alici, G. Bioinspired Three-Dimensional-Printed Helical Soft Pneumatic Actuators and Their Characterization. *Soft Robot.* **2020**, *7*, 267–282. [\[CrossRef\]](#)
19. Wallin, T.J.; Pikul, J.; Shepherd, R.F. 3D printing of soft robotic systems. *Nat. Rev. Mater.* **2018**, *3*, 84–100. [\[CrossRef\]](#)
20. Plott, J.; Shih, A. The extrusion-based additive manufacturing of moisture-cured silicone elastomer with minimal void for pneumatic actuators. *Addit. Manuf.* **2017**, *17*, 1–14. [\[CrossRef\]](#)
21. Schaffner, M.; Faber, J.A.; Pianegonda, L.; Rühls, P.A.; Coulter, F.; Studart, A.R. 3D printing of robotic soft actuators with programmable bioinspired architectures. *Nat. Comm.* **2018**, *9*, 878. [\[CrossRef\]](#)
22. Kalisky, T.; Wang, Y.; Shih, B.; Drotman, D.; Jadhav, S.; Aronoff-Spencer, E.; Tolley, M.T. Differential pressure control of 3D printed soft fluidic actuators. In Proceedings of the 2017 IEEE/RSJ International Conference on Intelligent Robots and Systems (IROS), Vancouver, BC, Canada, 24–28 September 2017; pp. 6207–6213.
23. MacCurdy, R.; Katzschmann, R.; Youbin, K.; Rus, D. Printable hydraulics: A method for fabricating robots by 3D co-printing solids and liquids. In Proceedings of the 2016 IEEE International Conference on Robotics and Automation (ICRA), Stockholm, Sweden, 16–21 May 2016; pp. 3878–3885.

24. Peele, B.N.; Wallin, T.J.; Zhao, H.; Shepherd, R.F. 3D printing antagonistic systems of artificial muscle using projection stereolithography. *Bioinspir. Biomim.* **2015**, *10*, 055003. [[CrossRef](#)] [[PubMed](#)]
25. Kang, H.-W.; Lee, I.H.; Cho, D.-W. Development of a micro-bellows actuator using micro-stereolithography technology. *Microelectron. Eng.* **2006**, *83*, 1201–1204. [[CrossRef](#)]
26. Truby, R.L.; Lewis, J.A. Printing soft matter in three dimensions. *Nature* **2016**, *540*, 371–378. [[CrossRef](#)] [[PubMed](#)]
27. Lee, S.; Jung, W.; Ko, K.; Hwang, Y. Wireless Micro Soft Actuator without Payloads Using 3D Helical Coils. *Micromachines* **2022**, *13*, 799. [[CrossRef](#)] [[PubMed](#)]
28. Jung, W.; Lee, S.; Hwang, Y. Truly 3D microfluidic heating system with iterative structure of coil heaters and fluidic channels. *Smart Mater. Struct.* **2022**, *31*, 035016. [[CrossRef](#)]
29. Tawk, C.; Alici, G. A Review of 3D-Printable Soft Pneumatic Actuators and Sensors: Research Challenges and Opportunities. *Adv. Intell. Syst.* **2021**, *3*, 2000223. [[CrossRef](#)]
30. Yang, D.; Verma, M.S.; So, J.-H.; Mosadegh, B.; Keplinger, C.; Lee, B.; Khashai, F.; Lossner, E.; Suo, Z.; Whitesides, G.M. Buckling Pneumatic Linear Actuators Inspired by Muscle. *Adv. Mater. Technol.* **2016**, *1*, 1600055. [[CrossRef](#)]
31. Yang, D.; Verma, M.S.; Lossner, E.; Stothers, D.; Whitesides, G.M. Negative-Pressure Soft Linear Actuator with a Mechanical Advantage. *Adv. Mater. Technol.* **2017**, *2*, 1600164. [[CrossRef](#)]
32. Zhang, C.; Zhu, P.; Lin, Y.; Jiao, Z.; Zou, J. Modular Soft Robotics: Modular Units, Connection Mechanisms, and Applications. *Adv. Intell. Syst.* **2020**, *2*, 1900166. [[CrossRef](#)]
33. Phillips, B.T.; Becker, K.P.; Kurumaya, S.; Galloway, K.C.; Whittredge, G.; Vogt, D.M.; Teeple, C.B.; Rosen, M.H.; Pieribone, V.A.; Gruber, D.F. A dexterous, glove-based teleoperable low-power soft robotic arm for delicate deep-sea biological exploration. *Sci. Rep.* **2018**, *8*, 14779. [[CrossRef](#)]
34. Zhou, Y.; Jin, H.; Liu, C.; Dong, E.; Xu, M.; Yang, J. A novel biomimetic jellyfish robot based on a soft and smart modular structure (SMS). In Proceedings of the 2016 IEEE International Conference on Robotics and Biomimetics (ROBIO), Qingdao, China, 3–7 December 2016; pp. 708–713.
35. Zhang, Y.; Zheng, T.; Fan, J.; Li, G.; Zhu, Y.; Zhao, J. Nonlinear Modeling and Docking Tests of a Soft Modular Robot. *IEEE Access* **2019**, *7*, 11328–11337. [[CrossRef](#)]
36. Jiao, Z.; Zhang, C.; Wang, W.; Pan, M.; Yang, H.; Zou, J. Advanced Artificial Muscle for Flexible Material-Based Reconfigurable Soft Robots. *Adv. Sci.* **2019**, *6*, 1901371. [[CrossRef](#)]
37. Zou, J.; Lin, Y.; Ji, C.; Yang, H. A reconfigurable omnidirectional soft robot based on caterpillar locomotion. *Soft Robot.* **2018**, *5*, 164–174. [[CrossRef](#)]
38. Meng, C.; Xu, W.; Li, H.; Zhang, H.; Xu, D. A new design of cellular soft continuum manipulator based on beehive-inspired modular structure. *Int. J. Adv. Robot. Syst.* **2017**, *14*, 1729881417707380. [[CrossRef](#)]
39. Tawk, C.; Panhuis, M.I.H.; Spinks, G.M.; Alici, G. Bioinspired 3d printable soft vacuum actuators for locomotion robots, grippers and artificial muscles. *Soft Robot.* **2018**, *5*, 685–694. [[CrossRef](#)]
40. Ashe, J. A New Bush Viper. *J. East Afr. Nat. Hist.* **1968**, *1968*, 53–59. [[CrossRef](#)]
41. Groen, J.; Bok, B.; Tiemann, L.; Verspui, G.J. Geographic range extension of the rough-scaled bush viper, *Atheris hispida* (Serpentes: Viperidae) from Uganda, Africa. *Herpetol. Notes* **2019**, *12*, 241–243.
42. Larson, K. *Can You Estimate Modulus from Durometer Hardness for Silicones*; Dow Corning Corporation: Midland, MI, USA, 2016; pp. 1–6.
43. Chung, S.M.; Yap, A.U.J.; Koh, W.K.; Tsai, K.T.; Lim, C.T. Measurement of Poisson's ratio of dental composite restorative materials. *Biomaterials* **2004**, *25*, 2455–2460. [[CrossRef](#)]

Disclaimer/Publisher's Note: The statements, opinions and data contained in all publications are solely those of the individual author(s) and contributor(s) and not of MDPI and/or the editor(s). MDPI and/or the editor(s) disclaim responsibility for any injury to people or property resulting from any ideas, methods, instructions or products referred to in the content.